Emittance and Current of Electrons Trapped in a Plasma Wakefield Accelerator

N. Kirby[*], I. Blumenfeld[*], C.E. Clayton[†], F.J. Decker[*], M.J. Hogan[*], C. Huang[†], R. Ischebeck[*], R.H. Iverson[*], C. Joshi[†], T. Katsouleas[**], W. Lu[†], K.A. Marsh[†], S. Martins[‡], W.B. Mori[†], P. Muggli[**], E. Oz[**], R.H. Siemann[*], D.R. Walz[*] and M. Zhou[†]

[*]Stanford Linear Accelerator Center, Stanford University, Stanford, California 94305, USA
[†]University of California, Los Angeles, California 90095, USA
[**]University of Southern California, Los Angeles, California 90089, USA
[‡]GoLP/IPFN, Instituto Superior Técnico, Portugal

Abstract. In recent experiments plasma electrons became trapped in a plasma wakefield accelerator (PWFA). The transverse size of these trapped electrons on a downstream diagnostic yields an upper limit measurement of transverse normalized emittance divided by peak current, $\varepsilon_{N,x}/I$. The lowest upper limit for $\varepsilon_{N,x}/I$ measured in the experiment is $1.3 \cdot 10^{-10} m/A$.

**Keywords:** Electron, Trapping, Plasma Wakefield Accelerator
PACS: 52.35.Py, 52.40.Mj, 41.75.Lx

In this experiment, ultrarelativistic electron drive bunches field ionized neutral vapor, creating a plasma [1] and expelling the plasma electrons from the bunch axis. The ions then pulled the plasma electrons back to the bunch axis with a time scale set by the inverse of the plasma frequency, $\omega_p = \sqrt{n_p e^2/(m\varepsilon_0)}$, where n_p, e, m, and ε_0 are the plasma density, the electron charge magnitude, the electron mass, and the permittivity of free space. The resulting plasma wake could accelerate some plasma electrons from rest to relativistic energies before they slipped out of the wake, trapping bunches of electrons. This process can produce electron bunches with small emittance and high peak current. Direct measurements of the trapped electron emittance and peak current were not possible; however, the ratio of these quantities is experimentally accessible. This paper presents a measurement of transverse emittance divided by peak current.

This experiment took place in the Final Focus Test Beam facility, located at the end of the Stanford Linear Accelerator Center linac. Let the quantities x and y represent the transverse coordinates and z denotes the longitudinal coordinate. Electron drive bunches of 3 nC and 42 GeV with normalized emittances of $\varepsilon_{N,x} = 60$ μm and $\varepsilon_{N,y} = 7$ μm, transverse sizes of 10 μm, and longitudinal bunch lengths of tens of μm entered a heat-pipe oven [2]. This heat-pipe oven confined lithium vapors of density, n_p, equal to $2.7 \cdot 10^{23}$ m^{-3} with a helium buffer gas. The lithium density was uniform in the middle of the oven, had a full width at half max (fwhm) length of 85 cm, and had Gaussian roll-offs at its up and downstream edges: $n_p \propto \exp(-(z-z_0)^2/(2\sigma_L^2))$, where $z - z_0$ denotes the distance from the edge of the uniform region and $\sigma_L = 3.97$ cm. Figure 1 displays the partial pressures of the two gas species in the heat-pipe oven. Beryllium windows of thickness 50 and 75 μm were located up and downstream of
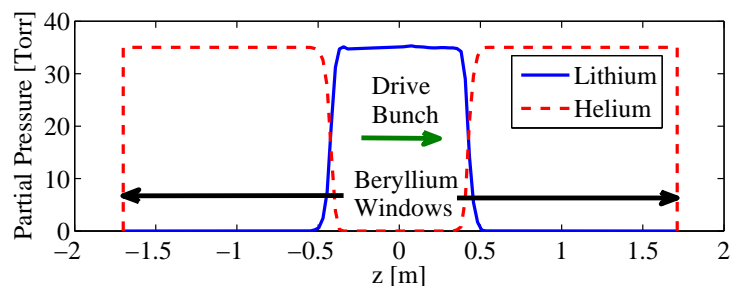
FIGURE 1. The partial pressure of helium and lithium in the heat-pipe oven. Beryllium windows created a boundary between the helium buffer gas and the beam line vacuum.

the plasma oven, respectively, and created boundaries between the buffer gas and the beam line vacuum. Downstream of the bunch-plasma interaction region the electrons passed through an energy spectrometer, which consisted of a magnetic dipole, two air gaps, and two cameras [3]. The positions of the two air gaps corresponded to low and high dispersion. One of the positions had higher energy resolution and the other had a broader energy range [4]. Figure 2 illustrates the experimental setup.
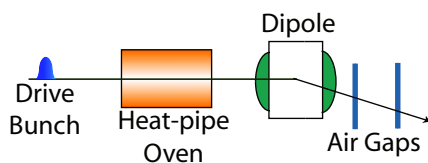

**FIGURE 2.** An illustration of the experimental setup.

The dipole dispersed electrons in the *y* direction according to their energy, which allowed for the measurement of the *x* root mean square (rms) size in the air gap, σ, as a function of energy. For most of the experiment the dipole had $\int B \cdot dl = 1.2$ or 0.27 Tm; however, for several data sets the dipole strength was varied, where it had a minimum value of $\int B \cdot dl = 0.016$ Tm. The corresponding minimum measurable energies were 11, 2.3, and 0.14 GeV, respectively. Figure 3 displays a sample image from the broad energy range air gap. The trapped electrons appeared on the energy spectrometer with transverse sizes much smaller than the drive bunch. Figure 4 shows an average energy spectrum of the trapped electrons.

An examination of the trapped electron propagation from the heat-pipe oven to the energy spectrometer reveals the connection between σ and $\varepsilon_{N,x}/I$. Earlier efforts treated the Gaussian density roll-off of the lithium as a tapering quadrupole focusing element, assuming no ionization of the helium buffer gas [5]. Under this assumed propagation model, the trapped electrons appear to achieve emittances better than 1 μm with spot sizes that are matched to the plasma [6]. A comparison between these conclusions and measurements from the energy spectrometer results in self-consistency problems: the trapped electrons were capable of ionizing helium.

The following sections show how the measurement of trapped electron properties changes in the presence of helium ionization. First, there is an overview of the requirements to ionize helium. Then, simulations and charge measurements from the energy
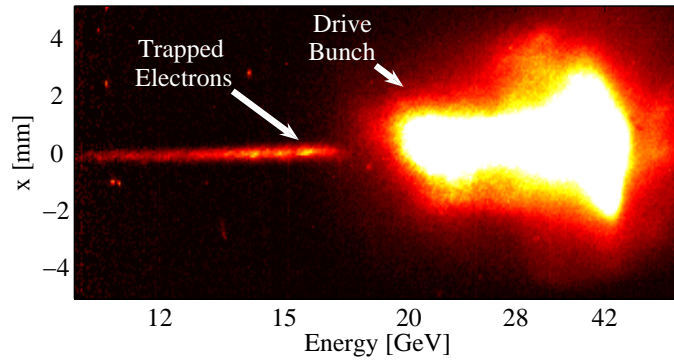
FIGURE 3. A saturated image of a drive bunch and trapped electrons from the energy spectrometer.
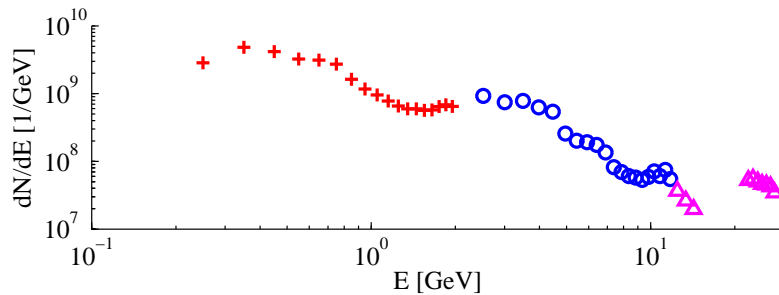
FIGURE 4. An averaged energy spectrum of the trapped electrons corresponding to drive bunches with peak currents in the range of 14.9 to 18.4 kA. The plus signs, circles, and triangles represent the data from the low dipole setting ($\int B \cdot dl \geq 0.016$ Tm), the broad energy range air gap, and the high energy resolution air gap, respectively.

spectrometer combine to show that the trapped electrons satisfied these requirements. Finally, upper bounds on the trapped electron bunch transverse and angular size, at the point it started to diverge freely, yield an upper limit measurement of $\varepsilon_{N,x}/I$.

Ionization depends heavily on the applied electric field: small increases in the electric field lead to large increases in the ionization rate [7] [8]. The probability of ionization depends on the ionization rate and the duration of the applied field. Gaussian bunches with $\sigma_z = 0.5, 1.9$, and 5 μm have a 0.5 probability of helium ionization with peak electric fields of 113, 95.7, and 86.1 GV/m, respectively. Despite an order of magnitude increase in the bunch length, from 0.5 to 5 μm, the electric field required for ionization only decreases by 24%. The peak electric field of an electron bunch with $\sigma_x = \sigma_y$ is proportional to I/σ_x, where σ_x and σ_y represents its x and y rms size, respectively. For a given longitudinal bunch length, the maximum transverse size capable of ionizing helium, σ_m, is proportional to the peak current: $\sigma_m = \alpha I$; here α is the proportionality constant when the ionization probability at the peak field position of a Gaussian bunch is equal to 0.5. Due to the high sensitivity of the ionization rate to the electric field, the quantity α is only weakly dependent on the bunch length: for $\sigma_z = 0.5, 1.9$, and 5 μm, $\alpha = 2.39, 2.83$, and $3.14 \cdot 10^{-10}$ m/A, respectively.

Plasma electron trapping occurs only in regions where both lithium and helium are

present [9]. Thus, electron trapping happened in both the up and the downstream transition regions between the gas species; the electrons trapped in these different regions had different properties. Lithium ionization (5.4 eV) occurred first and set up the plasma wake. The higher ionization energy of helium (24.6 eV) allowed some of its electrons to satisfy the trapping criterion [9]. As the drive bunch traversed the heat-pipe oven, electrons became trapped in small regions at the back of the accelerating portions of the wake. In the upstream boundary, the plasma wavelength shortened as the drive bunch traversed the boundary. Electrons trapped at densities significantly lower than $2.7 \cdot 10^{23}$ m^{-3} ended up in the decelerating part of the wake as the plasma wavelength shortened, so they didn't remain trapped. Thus, the upstream trapped electrons had small longitudinal bunch lengths. In addition, these electrons accelerated throughout the 85 cm of lithium, which allowed some of these to obtain high energies ($\approx$30GeV). The same was not true for the trapped electrons from the downstream boundary. There, the plasma wavelength increased as the drive bunch traversed the boundary. In comparison to the upstream electrons, the downstream trapped electrons were low energy and had large longitudinal bunch lengths.

Three dimensional full particle in cell simulations with the code OSIRIS [10] provided the basic length scale of the trapped electrons. These simulations were for Gaussian drive bunches with $1.8 \cdot 10^{10}$ electrons, $\sigma_{x,y} = 1.74$ μm, σ_z varied from 10 to 50 μm in 10 μm steps, and represent the experimental drive bunches. To approximate the region of the upstream boundary where trapping occurs, the lithium density was set to its maximum, $2.7 \cdot 10^{23}$ m^{-3}, with a small background helium density of $8.1 \cdot 10^{21}$ m^{-3}. In x, y, and z, the simulation grid size was $1/2$ μm with either 2 or 4 particles per cell. Second order particle shapes were used to reduce numerical noise and improve energy conservation [11]. The trapped electron bunches had longitudinal fwhm lengths ranging from 2.7 to 6.3 μm, which correspond to Gaussian bunches with $\sigma_z = 1.1$ and 2.7 μm, respectively. Since $\sigma_z = 1.9$ μm is in the middle of the simulation range, the corresponding value of $\alpha = 2.83 \cdot 10^{-10}$ m/A is most appropriate for describing the experiment. The simulations did not include the Gaussian roll-offs of the heat-pipe oven, so the longitudinal characteristics from the simulations are only representative of the trapped electrons from the upstream boundary.

A combination of the simulation results and charge measurements of the upstream trapped electrons shows that the trapped electrons were capable of ionizing helium. The energy spectrum includes electrons from both the up and the downstream boundaries, but the latter could not reach energies as high as the former. Let E_m denote the maximum energy achievable for the downstream trapped electrons. An integral of the accelerating field scale, $mc\omega_p/e \ (\sqrt{mc^2 n_p(z)/\varepsilon_0})$, over the downstream lithium density profile yields E_m as

$$E_m = e\sqrt{mc^2 n_p(z_0)/\varepsilon_0} \int_{z_0}^{\infty} \exp(\frac{-(z-z_0)^2}{4\sigma_L^2})dz = 3.5 GeV, \tag{1}$$

where c is the speed of light. As the plasma wavelength increased, the position of the maximum accelerating field changed. Equation 1 ignores this effect, but is still useful for setting a scale for E_m. An integration of averaged, trapped electron energy profiles above 3.5 GeV for drive bunch peak currents in the intervals of 8.3 to 11.0, 11.0 to 13.2, 13.2 to 15.1, 15.1 to 16.8, and 16.8 to 18.4 kA shows that the upstream trapped

electrons had more than 1.34, 1.67, 1.65, 1.90, and 2.06·10^9 electrons, respectively. The matched transverse size for a 3.5 GeV electron bunch with $\varepsilon_{N,x} = 1.0$ μm is 0.42 μm; it is smaller for higher energies. A Gaussian bunch with 1.34·10^9 electrons and $\sigma_x = \sigma_y$ = 0.42 μm stops ionizing helium when its $\sigma_z \geq 17$ μm, which is an order of magnitude larger than the simulations indicate. An analysis of the trapped electron properties when assuming no helium ionization yields the conclusion that the trapped electrons could ionize helium. This is a proof by contradiction of the helium ionization. In addition the drive bunches, if properly matched to the plasma, were also capable of ionizing the helium. Thus, the helium buffer gas is an important factor in the propagation of the trapped electrons to the energy spectrometer.

An upper limit measurement of $\varepsilon_{N,x}/I$ results from the determination of upper bounds on the trapped electron bunch transverse and angular size at the point it started to diverge freely. The trapped electrons diverged freely either before or when they reached the downstream beryllium window. The size on the broad energy range air gap, σ, divided by the length from the beryllium window to this air gap, L=193cm, is an upper limit measurement of the angular divergence.

Ionization of helium created an ion column that was capable of confining an electron bunch transversely in the buffer gas. The driver of the helium wake was subject to head erosion: the front of the bunch didn't experience a focusing field so it expanded, which caused the front of ionization to move further into the bunch [12]. An earlier section indicates that both the drive and trapped bunches were capable of ionizing helium. In order for the trapped electrons to have diverged before they reached the downstream beryllium window, the ionization front had to move through both the drive and trapped bunch. A bunch that was too large transversely to ionize helium would have diverged freely. Thus, the maximum size the trapped bunch could have been at the point they started to diverge freely was $\sigma_m = \alpha I$.

Equation 2 expresses the transverse normalized emittance.

$$\varepsilon_{N,x} = \gamma\sqrt{\langle x^2 \rangle \langle \dot{x}^2 \rangle - \langle x\dot{x} \rangle^2}. \tag{2}$$

The quantity $\dot{x}$ denotes dx/dz. Until the bunches began to diverge freely, the $x\dot{x}$ correlation term was small. An inequality then replaces Eq. 2.

$$\varepsilon_{N,x} < \gamma\sigma_x\sigma_{\dot{x}}, \tag{3}$$

where $\sigma_{\dot{x}}$ represents the rms size of the bunch in $\dot{x}$. The substitution of σ_m and σ/L into the upper limit for emittance results in an upper limit measurement of $\varepsilon_{N,x}/I$, shown in Eq. 4.

$$\frac{\varepsilon_{N,x}}{I} < \frac{\gamma\alpha\sigma}{L}. \tag{4}$$

The trapped electrons appeared with sizes near the camera resolution [5]. Thus, as γ increases so does the upper limit of $\varepsilon_{N,x}/I$; this is a consequence of a fixed camera resolution instead of a property of the trapped electrons. In addition, the trapped electrons drove a decelerating helium wake, so electrons at lower energies were originally at higher energies. This makes the upper limit for $\varepsilon_{N,x}/I$ of the low energy electrons also representative of the higher energy electrons. The broad energy range air gap was

capable of measuring electrons at lower energies, so measurements of σ came from this diagnostic.

Measurement uncertainties are dominated by systematic errors. The definition of α corresponds to a bunch with $\sigma_z = 1.9\ \mu$m and ionization probability at its peak field position equal to 0.5. If the trapped bunch lengths varied over the same range displayed in the simulations, it would lead to as much as a 6% error in α. In addition, the definition of α by a 0.5 ionization probability is somewhat arbitrary. Determining α by a 0.1 ionization probability results in a 22% growth of α; however, simulations using the code QuickPIC [13] indicate that the 0.5 probability condition is more than sufficient in defining the maximum trapped electron bunch size. Other systematic errors are introduced by the camera resolution and the neglect of the $x\dot{x}$ correlation term; both of these terms result in an overestimate of $\varepsilon_{N,x}/I$. The errors result in a measurement that is systematically larger than the actual $\varepsilon_{N,x}/I$: the measurement for $\varepsilon_{N,x}/I$ is a true upper limit.

The focusing properties of the heat-pipe oven's helium buffer gas are an important factor in determining the propagation to the energy spectrometer. Requirements for helium ionization set a maximum transverse size for the trapped electrons when they began to diverge freely. A combination of this maximum size with the final angular divergence of the trapped electrons yields an upper limit measurement of $\varepsilon_{N,x}/I$. The lowest upper limit for $\varepsilon_{N,x}/I$ measured in the experiment is $1.3 \cdot 10^{-10} m/A$.

REFERENCES

1. C. L. O'Connell, et al., *Physical Review Special Topics - Accelerators and Beams* **9**, 101301 (2006).
2. P. Muggli, et al., *IEEE Transactions on Plasma Science* **27**, 791 (1999).
3. N. Kirby, et al., "Energy Measurements of Trapped Electrons from a Plasma Wakefield Accelerator," in *Advanced Accelerator Concepts*, 2006, p. 541.
4. R. Ischebeck, et al., "Energy Measurements in a Plasma Wakefield Accelerator," in *Proceedings of PAC*, 2007, p. 4168.
5. N. Kirby, et al., "Emittance Measurements of Trapped Electrons from a Plasma Wakefield Accelerator," in *Proceedings of PAC*, 2007, p. 4183.
6. K. A. Marsh, et al., "Beam Matching to a Plasma Wake Field Accelerator using a Ramped Density Profile at the Plasma Boundary," in *Proceedings of PAC*, 2005, p. 2702.
7. M. V. Ammosov, N. B. Delone, and V. P. Krainov, *Sov. Phys. JETP* **64**, 1191 (1986).
8. D. L. Bruhwiler, et al., *Physics of Plasmas* **10**, 2022 (2003).
9. E. Oz, et al., *Physical Review Letters* **98**, 084801 (2007).
10. R. A. Fonseca, et al., "OSIRIS: A Three-Dimensional, Fully Relativistic Particle in Cell Code for Modeling Plasma Based Accelerators," in *Proceedings of the International Conference on Computational Science-Part III*, 2002, p. 342.
11. T. Esirkepov, *Computer Physics Communications* **135**, 144–153 (2001).
12. I. Blumenfeld, et al., *Nature* **445**, 741–744 (2007).
13. C. Huang, et al., *Journal of Computational Physics* **217**, 658 (2006).